

The Effect of Resolution on Terrain Feature Extraction

S. T. Arundel

U.S. Geological Survey
Center of Excellence for Geospatial Information Science
Rolla, MO
sarundel@usgs.gov

Wenwen Li, Xiran Zhou

School of Geographical Sciences & Urban Planning
Arizona State University
Tempe, AZ
{wenwen, xrzhou}@asu.edu

Abstract—Recent increase in the production of high-resolution digital elevation models (DEMs) from lidar data has led to interest in their use for terrain mapping. Although the impact of different resolutions has been studied relative to terrain characteristics like roughness, slope and curvature, its relationship to the extraction of terrain features remains unclear. To address this question, this study tests the impact of four resolutions on the capture of glacial cirques from DEMs. Mean curvature was derived from one arc-second, one-third arc-second, one-ninth arc-second and half meter DEMs representing a cirque-covered mountainous region southwest of Lake Tahoe, California. Using a GEOBIA workflow, ridge objects were identified, and three scales - via the multi-resolution scale parameter (SP) - of objects bordering the ridges were classified as cirque objects. The resulting classifications were compared to reference cirques digitized at a scale of ~1:10,000. Results show that the one-third arc-second DEM produces the set of cirque objects most closely resembling the reference cirques. The one-ninth arc-second DEM afforded the second-best classification. These results emphasize the importance in carefully choosing resolution relative to the features extracted, rather than using the highest resolution data available. In the case of GEOBIA workflows, the choice of scale parameter is equally important.

I. INTRODUCTION

The growing accessibility of digital elevation models at increasingly higher resolution, and continued improvements in computing power and modelling software are encouraging unprecedented opportunities for geomorphologists to make advances in landform mapping [1]. Automatic classification of surface shapes fosters more objective portrayal of forms and, particularly, their boundaries. While accuracy may also be increased, the introduction of error by automation must be minimized through the proper choice of classification (and partitioning) algorithms, study area size, collection scales and DEM resolutions (grid cell size).

Most terrain *attributes* derived directly from DEM cell values, like slope and curvature, are known to vary with changing DEM resolutions [2], and many efforts to automate landform classification depend upon the inferred relationship between

different terrain attributes and erosional or depositional processes [3]. However, the approach of classifying these attributes on a cell by cell basis is constraining in various features, including difficulty in capturing topological relationships between landscape objects and referencing the scale of analysis to the raster resolution. Geographic object-based image analysis (GEOBIA), in which the cell-based dataset is segmented into elementary forms before classification is a suggested approach employed to overcome these limitations [4]. However, the impact of changing DEM resolution on terrain *objects* and their classification should be better understood, as choice of resolution is an important step in processing data.

This paper assesses how object representation of one specific landform type (glacial cirques) changes with four increasingly larger resolutions of DEMs produced from the same lidar dataset. The cirque objects are created using basic semantics and GEOBIA technology, and tested against a reference dataset.

Cirques as landforms offer an ideal test case because of their characteristic topographic signature in mountainous regions [5]. Cirque delineation is fairly straight-forward in areas where they are clearly defined, making them good automated test features, and identifiable as amphitheatre-like depressions in alpine glacial terrain. Because cirque sizes studied across several regions vary from about 6 to 10 hectares (15 to 25 acres) [6], objects smaller than 10 acres were not analysed in this study.

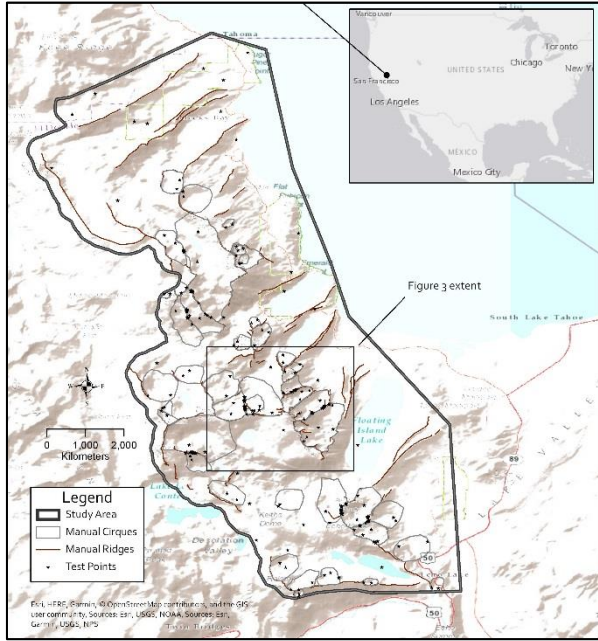
II. STUDY AREA

The study area is composed of a 10,000-km² area in the east-central Sierra Nevada mountain range located just west and southwest of Lake Tahoe (Figure 1). Elevation ranges in the study area from 1798 m above sea level (a.s.l.) to 3043 m a.s.l.

The Sierra Nevada mountain range is the longest and highest in the coterminous United States. The backbone of the range is mostly Mesozoic granite, formed where a chain of volcanoes intruded into the older Palaeozoic rock. By the Late Cretaceous, the deep granite had been uncovered by erosion. The range developed as either the eastern basin subsided, or the exposed

88 granite was uplifted along a north-south fault east of the range [7].
 89 The study area exhibits numerous cirques and other typical glacial
 90 features like arêtes, tarns, and glacial moraines as evidence of
 91 glacial erosion. As of 2008, over 100 glaciers still existed in the
 92 Sierra Nevada mountains [8].

93



94

95 Figure 1. Study area in the east-central Sierra Nevada mountains, showing
 96 hand-drawn ridges, glacial cirques, and stratified random test points.

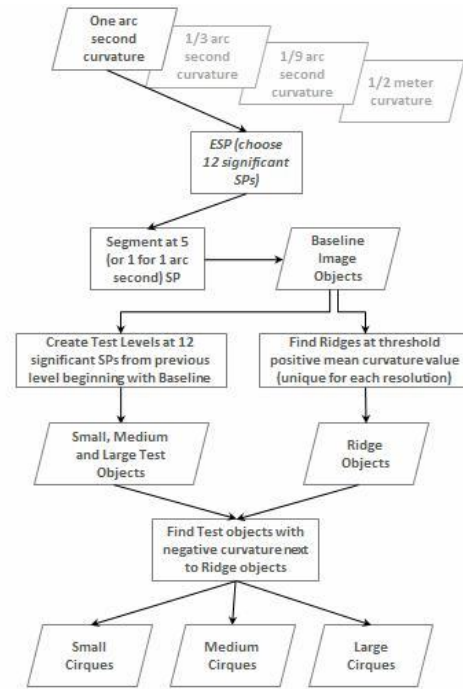
97 In August of 2010, lidar data were collected for the Tahoe
 98 Basin, with an average native pulse density of > 8 pulses per square
 99 meter over terrestrial surfaces. The data delivered to the US
 100 Geological Survey (USGS) from this collection included point
 101 clouds with an average ground point density of 2.26 points per
 102 square meter, and a half-meter resolution DEM that was
 103 incorporated into The National Map's (TNM) one-ninth (1/9) -,
 104 one-third (1/3) - and one - arc-second datasets. Although the 1/2 m
 105 DEMs were not integrated into the new 3DEP 1-m dataset that was
 106 not yet in production, they are available for download from TNM
 107 as the Original Product Resolution (OPR) data. The availability of
 108 a range of resolutions allows analysis of the impact these
 109 resolutions have on feature delineation and classification. All
 110 specifications related to both lidar and DEM data products can be
 111 accessed
 112 https://nationalmap.gov/3DEP/3dep_prodstandards.html.

113

III. METHODS

114 The semantics-based glacial cirque classification workflow is
 115 based on that developed for a test region in Austria [9]. The results
 116 and detailed methods of a modified workflow tested in the study
 117 area are reported by [10].

118 The same general steps are followed for each of the four DEM
 119 resolutions (Figure 2). First, a mean curvature raster is derived
 120 from the study area (plus buffer) DEM. Baseline objects are then
 121 created in a GEOBIA software (Trimble® eCognition®) using the
 122 multiresolution segmentation (MRS) algorithm, setting the scale
 123 parameter (SP) to 5 for all resolutions except the 1 arc-second
 124 dataset, for which an SP of 1 was required to generate sufficiently
 125 small objects for future segmentation and classification. Baseline
 126 objects were classified as ridges if mean curvature exceeded a
 127 manually selected threshold value.



128

129

130

Figure 2. Workflow for producing three cirque sizes from four DEM resolutions.

131 Non-ridge objects were then segmented at consecutive SPs as
 132 specified by the Estimation of Scale Parameter tool [11] to create
 133 12 test object levels. Objects in the test levels were classified as
 134 cirques where they had a negative mean curvature (concave), and
 135 bordered a ridge object. Adjacent cirque objects were then merged
 136 together and those smaller than 10 acres (~40,000 m²) removed
 137 from the cirque class. Because the size of cirques ranges from 15
 138 to 25 acres, three size levels were chosen from each resolution to

139 produce small, medium and large “cirque” datasets so that the
 140 choice of a single SP did not introduce unnecessary bias. The
 141 resulting ridge and cirque objects were compared visually and
 142 statistically to a separate reference dataset manually circumscribed
 143 at the USGS and Arizona State University at a scale of ~1:10,000.

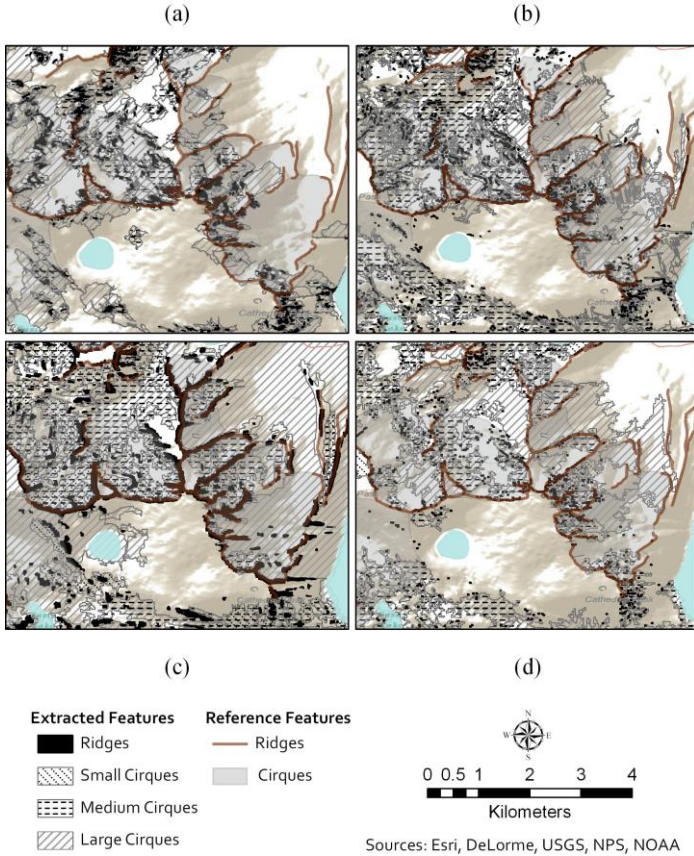


Figure 3. Ridges and cirques extracted from the 3DEP one arc-second resolution (Figure 3a), one-third arc-second resolution (Figure 3b), one-ninth arc-second resolution (Figure 3c), and one-half meter resolution (Figure 3d) DEMs using the GEOBIA workflow.

IV. RESULTS AND DISCUSSION

A. Visual assessment

147 A smaller region around Mt Tallac, California, was used for
 148 the visual assessment, as it contains many cirques within a small
 149 area. Ridge extraction from the lowest resolution dataset (one arc-
 150 second, see Figure 3a) was fairly poor, and in many cases ridges
 151 are represented by disconnected objects, often just a few grid cells
 152 or less in size. This is likely caused by too large of a cell size of
 153 the DEM relative to the narrow width of ridges. Considering this
 154 shortcoming, extracted cirque features, particularly the large ones
 155 (run at high SP) resemble reference cirques remarkably well. The

156 representation appears to fail greatest in classifying non-cirque
 157 objects as cirque objects (false positives), rather than in
 158 misclassifying cirque objects as non-cirque (false negatives).

159 Ridges derived from the one-third arc-second resolution DEM
 160 quite closely resemble the reference ridges (Figure 3b). Classified
 161 cirque objects match those of the reference cirques well, although
 162 in many cases they fail to capture the full extent of the cirque,
 163 increasing the number of false negatives. The classification, in
 164 general, displays fewer false positives than does the one arc-
 165 second classification.

166 Ridges classified from the one-ninth arc-second resolution
 167 DEM fail to match reference ridges well (Figure 3c). In particular,
 168 they are less linear and extensive. The classified cirques are more
 169 closely matched in extent to the reference cirques than those of the
 170 one-third arc-second DEM, particularly those created using the
 171 large SP. The classification generally exhibits more false positives,
 172 particularly in the southwest corner of the figure, than the one-third
 173 arc-second classification, but fewer false negatives than the one
 174 arc-second classification.

175 Ridges extracted from the half-meter DEM (Figure 3d) are
 176 similar to those of the one-ninth arc-second dataset. Cirque objects,
 177 however, fall short of the reference dataset, particularly along the
 178 northeast side of Mt Tallac where many large cirques exist in the
 179 reference dataset. False positive objects are seen in the
 180 southwestern part of the figure like the one-ninth arc-second
 181 extraction, but are not as extensive.

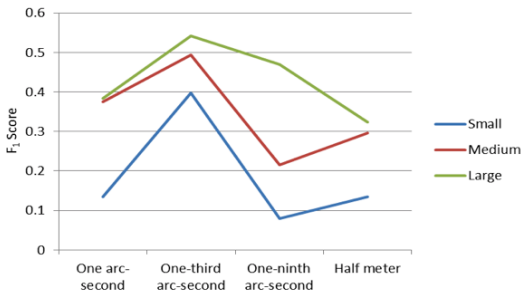
B. Statistical assessment

183 Five hundred random, stratified test points were generated
 184 automatically, and were assigned a value of 1 where they fell
 185 within a cirque and 0 where they did not (Figure 1). F₁ score was
 186 employed to compare the classification accuracy using different
 187 DEMs. This score is a quantitative measure based on the precision
 188 and recall of the classification relative to the reference dataset.
 189 Precision in our application measures the ratio of correctly
 190 classified cirque points over all points that have been classified as
 191 cirque points. Recall measures the ratio between correctly
 192 classified cirque points over all true cirque points. Mathematically,
 193 the F₁ score can be expressed as:

$$F^1 = 2 \times \frac{1}{\frac{1}{recall} + \frac{1}{precision}} = 2 \times \frac{precision \times recall}{precision + recall}$$

195 Figure 4 demonstrates the F₁ scores for the retrieval of cirques
 196 at different sizes. F₁ scores indicate that the one-third arc-second
 197 resolution DEM produces the best results in all three cirque sizes.
 198 The one-ninth arc-second DEM produced large objects with good
 199 results, and the one-arc second DEM produced large and medium

200 objects with fair results. Interestingly, results were increasingly
 201 better from small to large objects for each resolution.



202 Figure 4. F₁ scores for three cirque sizes across four DEM resolutions.

204 The fact that the one-third arc-second dataset provided the best
 205 resolution to reproduce the reference dataset is likely due to (at
 206 least) two reasons. First, the grid cell size itself is likely to be
 207 well-suited to the size of the natural features (cirques) themselves.
 208 Smaller cells tend to produce more noise not related to the features
 209 of interest. Larger cells, on the other hand, may smooth the DEM
 210 to the point of missing areas of extreme curvature. Secondly, the
 211 scale at which the reference features were digitized (1:10,000) falls
 212 between the working scales of the one-third (~1:24,000) and the
 213 one-ninth (~1:8,000), which might help explain why the one-ninth
 214 arc-second also performed well. It would be interesting to test the
 215 results relative to reference features derived at different scales,
 216 although such an approach would likely not be feasible in a real
 217 extraction case, as creating just one reference dataset is often too
 218 costly. In any case, the scale at which reference features are created
 219 should be taken into consideration when evaluating statistical
 220 comparisons between them and extracted features.

221 The variation in fit between extracted and reference features
 222 based on cirque size (scale parameter) can be as pronounced as that
 223 based on DEM resolutions. In fact, the average range of object
 224 size-based F₁ scores (0.27) was greater than that of the resolution-
 225 based F₁ scores (0.24). This suggests that the choice of object size
 226 (scale parameter) is as important as, and possibly more important
 227 than, the choice of DEM resolution. Certainly, it appears that both
 228 should be considered carefully before modelling terrain features
 229 using object-based image analysis.

230 V. CONCLUSION

231 Study results indicate that differing DEM resolutions can
 232 greatly impact the accuracy of extracted terrain features such as
 233 glacial cirques. DEM resolutions of working scales close to the
 234 reference feature scale should be chosen, as well as cell sizes
 235 appropriate for mapping the proposed feature.

236 The chosen relative GEOBIA scale parameter was found to
 237 impact the accuracy of the extraction as much as does the DEM

238 resolution. Therefore, resolution and scale choices in terrain
 239 feature extraction using GEOBIA techniques are doubly
 240 complicated, and must be contemplated thoroughly and wisely.

241 This work could be improved by including additional study
 242 areas, and expand to a range of terrain features. Additionally, it
 243 would be interesting to test extractions against reference features
 244 generated at various scales, particularly if those scales can more
 245 closely match the DEM working scales.

246 ACKNOWLEDGMENT

247 This research was funded by the National Geospatial Program
 248 as part of the U.S. Geological Survey. "Any use of trade, firm, or
 249 product names is for descriptive purposes only and does not imply
 250 endorsement by the U.S. Government."

251 REFERENCES

- 252 [1] Drăguț, L., and C. Eisank, 2009. "Object representations at multiple scales
 253 from digital elevation models." *Geomorphology*, 129, 183–189.
- 254 [2] Huang, X., K. Liu and L. Xiong, 2015. "The Influence of DEM Resolution on
 255 the Extraction of Terrain Texture." *Geomorphometry*, 123–125.
- 256 [3] Csillik, O., I. S. Evans, and L. Drăguț, 2015. "Transformation (normalization)
 257 of slope gradient and surface curvatures, automated for statistical analyses
 258 from DEMs." *Geomorphology*, 232, 65–77.
- 259 [4] Minár, J., and I. S. Evans, 2008. "Elementary forms for land surface
 260 segmentation: The theoretical basis of terrain analysis and geomorphological
 261 mapping." *Geomorphology*, 95, 236–259.
- 262 [5] Tricart, J., and A. Cailleux, 1962. "Le modèle glaciaire et nival. *Inf. Geogr.*
 263 28, 221 (1962).
- 264 [6] Evans, I. S., and N. J. Cox, 2015. "Size and shape of glacial cirques:
 265 comparative data in specific geomorphometry." *Geomorphometry for*
 266 *Geosciences*. 63, 79–82 (2015).
- 267 [7] Henry, C. D., 2009. "Uplift of the Sierra Nevada, California." 575–576.
- 268 [8] Basagic, H. J. I., 2008. "Quantifying twentieth century glacier change in the
 269 Sierra Nevada, California." Portland State University.
- 270 [9] Eisank, C., L. Drăguț, J. Gotz, and T. Blaschke, 2015. "Developing a
 271 semantic model of glacial landforms for object-based terrain classification—
 272 the example of glacial cirques." *GEOBIA*, 1682-1777.
- 273 [10] Arundel, S. T., 2016. "Pairing semantics and object-based image analysis for
 274 national terrain mapping - a first-case scenario of cirques." *GEOBIA 2016 :
 275 Solutions and Synergies* (eds. Kerle, N., Gerke, M. & Lefevre, S.) (2016).
- 276 [11] Drăguț, L., D. Tiede, and S. R. Levick, 2010. "ESP: a tool to estimate scale
 277 parameter for multiresolution image segmentation of remotely sensed data."
 278 *Int. Journal of Geographical Information Science*, 24, 859-871.